J Oral Pathol Med (2004) 33: 543–9

www.blackwellmunksgaard.com/jopm

The involvement of $K_v3.4$ voltage-gated potassium channel in the growth of an oral squamous cell carcinoma cell line

Tien-Shen Lew[1], Che-Shoa Chang[2,3], Kung-Ping Fang[2], Chian-Yi Chen[1], Cheng-Hsiung Chen[1], Shu-Chun Lin[2]

[1]*Institute of Physiology and* [2]*School of Dentistry, National Yang-Ming University, Taipei;* [3]*Department of Dentistry, Veterans General Hospital-Taipei, Taipei, Taiwan*

BACKGROUND: In our previous study, an A-type voltage-gated K^+ channel, $K_v3.4$, was found more frequently expressed in oral squamous cell carcinoma (OSCC) when compared with non-cancerous matched oral tissue. An OSCC cell line, OECM-1, was found to have moderate level of $K_v3.4$ expression.

METHODS: To further elucidate the roles of $K_v3.4$ for the involvement of neoplastic process, we amplified $K_v3.4$ coding sequence by reverse transcriptase polymerase chain reaction (RT-PCR), constructed an expression vector carrying this sequence and then stably transfected into OECM-1 OSCC cells.

RESULTS: We demonstrated the integration and constitutive expression of $K_v3.4$ in the cell. A unique A-type current elicited by such expression in OECM-1 cells was defined by patch clamp analysis. This current pattern can be reversibly blocked by an A-type K^+ channel blocker 2 mM 4-aminopyridine (4-AP). The acquisition of $K_v3.4$ activity in OECM-1 cells bestowed growth advantage. However, in 3T3 cell, transfected $K_v3.4$ caused only limited increase of growth without forming transformation foci.

CONCLUSION: The present study established a stable keratinocyte system carrying functional $K_v3.4$ and increase of growth, by which the anti-$K_v3.4$ modalities for potential OSCC control can be further investigated.

J Oral Pathol Med (2004) **33**: 543–9

Keywords: $K_v3.4$; mouth; neoplasm; oral carcinoma; potassium channel

Potassium channels consist of multiple families, including voltage-gated K^+ channels (K_v) and inwardly rectifying K^+ channels (K_{ir}) (1). The major K_v family members include the shaker, ether-a-go-go (EAG), and potassium voltage-gated channel, KQT-like subfamily (KCNQ) subfamilies, as well as other subunits. All K_v members share similar transmembrane domains that form the K^+ conducting pore. The conduction of K^+ ion out of the cell should hyperpolarize the cell membrane. To maintain the resting potential, cell membrane needs to be hyperpolarized (2). The most N-terminal structure (inactivation domain) of K_v occludes the pore from the cytoplasm by a conformational switch. Conformational changes of the N-terminal end through phosphorylation or protein interaction can suppress the inactivation domain, allowing a longer time for K^+ transport (1). For instance, phosphorylation status of EAG-related (ERG) K_v modulated by *Src* tyrosine kinase and *Src* homology protein-1 (SHP-1) tyrosine phosphatase can regulate the current flux (3, 4).

In non-excitable cells, other than the role of maintaining membrane potential, K^+ channels may contributes to homeostasis, cell cycle regulation, differentiation and apoptosis (3, 4). It is also well-known that K^+ channels are involved in mitogenesis and volume regulation in lymphocytes (5). Regulation of growth by K^+ channels has been observed in a variety of malignant cells (6–8). In addition, aberrances in several K_v are present in multiple human primary neoplasms (6, 7, 9–11). Smith et al. (11) showed the selective up-regulation of *ERG* gene expression and function in a panel of hematopoietic neoplasms. Pardo et al. (12) have advanced further evidences that human EAG K_v plays a direct role in controlling proliferation and transformation of epithelial cells. The interaction between cytoskeleton and EAG K_v can affect the electrophysiological property of K_v at different cell cycle stage (13). Moreover, overexpression of GIRK1, a G protein-gated K_{ir}, in primary breast carcinomas has been reported as a useful biomarker for lymph node metastasis (14). Thereby, K^+ channels contributing to the neoplastic process might be served as potential markers for molecular staging and therapeutic targeting (11).

Disruption of $K_v3.4$ (also called *KCNC4*, *shaw III* or *Raw3*), a shaker-related K_v subfamily member, was involved in a human neuromuscular disease, periodic paralysis (15). $K_v3.4$ is an A-type K^+ channel

Correspondence: Shu-Chun Lin, Institute of Oral Biology, School of Dentistry, National Yang-Ming University, Li-Nong St, Sec. 2 No. 155, Peitou, Taipei, Taiwan 112. Fax: +8862-28264053, E-mail: sclin@ym.edu.tw
Accepted for publication March 10, 2004

characterized by a rapid inactivation of depolarized current through the occlusion of channel pore by inactivation domain. This channel has become a paradigm for understanding the inactivation domain in K_v (16). Tumor cells are highly depolarized (17). Expression of $K_v3.4$ in 64% oral squamous cell carcinoma (OSCC) in relation to the 29% in non-cancerous matched tissue (NCMT) was identified in our previous study (18). An increased expression of $K_v3.4$ was also noted in eight of 10 esophageal SCC (ESCC)/NCMT tissue pairs studied (18). The growth of OSCC cells was suppressed by the administration of 4-aminopyridine (4-AP), which is an A-type K^+ channel blocker. In this study, we have established an overexpression system and further identified the function of $K_v3.4$ in the growth of oral keratinocyte.

Materials and methods

Cell culture

The OECM-1 OSCC cell line was grown in RPMI 1640 (Life Tech., Gaithersburg, MD, USA) (19). The 3T3 cell clone A31-1-1 from mouse embryonic fibroblasts was grown in MEM (Life Tech.) (20). Heat inactivated fetal calf serum (FCS, 10%) was routinely supplemented to media except for occasional experimental demands. All media also contained 100 units/ml of penicillin plus 100 μg/ml streptomycin together with 0.25 μg/ml amphotericin B.

DNA and RNA isolation

Genomic DNA was isolated using a QIAamp kit (Qiagen, Hilden, Germany). Total RNA was isolated from lytic cells using a PureScript RNA isolation kit (Gentra, Minneapolis, MN, USA). The RNA was treated with DNAse I (Life Tech.) to remove the contaminated DNA.

Amplification of the coding sequence of $K_v3.4$

One microgram total RNA was converted to cDNA with SuperScript II reverse transcriptase (Life Tech.) and oligo-d$(T)_{18}$. cDNA equal to 100 ng total RNA was subjected to polymerase chain reaction (PCR) amplification. The entire coding sequence of $K_v3.4$ was amplified from cDNA of OECM-1 to produce a 1775-bp amplicon using primer pair 1 (Table 1).

Plasmid construction and transfection

After the $K_v3.4$ coding sequence was confirmed, the amplicon was cloned to a mammalian expression vector pcDNA3.1 (Invitrogen, Groningen, the Netherlands). The accuracy of the constructed plasmid was reconfirmed by restriction map analysis and sequencing. The constructed plasmid and empty vector were transfected using Geneporter I (Gene Therapy System, San Diego, CA, USA). At 48 h after the transfection, the medium was changed to include 0.3 mg/ml or 1.0 mg/ml geneticin (Life Tech.) for OECM-1 and 3T3 cell, respectively. In the third week, independent clones were isolated and expanded for analysis.

Determination of integration and mRNA expression

The integration and expression of $K_v3.4$ mRNA in stable clones was detected by PCR using exon spanning primer pair 2 (spanning $K_v3.4$ exons 1 and 2) in Table 1. To confirm the integration of exogenous $K_v3.4$ cDNA in OECM-1 cell, genomic DNA of stable clones was used as template. The expression of both endogenous $K_v3.4$ mRNA and exogenous $K_v3.4$ cDNA was assured by using cDNA of stable clones was used as a template. Amplification of β-actin was a control for efficiency of amplification. The sequences were as follows: sense – 5′-ACACTGTGCCCATCTACGAGG-3′ and antisense – 5′-AGGGGCCGGACTCGTCATACT-3′ (ass. no.: X00351).

Electrophysiological measurement

Patch-clamp recordings were obtained from synchronized OECM-1 cells treated with lovastatin (Sigma, St Louis, MO, USA) (21). The cells were placed in the recording chamber containing saline solution (140 mM NaCl, 5 mM KCl, 1 mM $MgCl_2$, 1 mM $CaCl_2$, 10 mM glucose, and 10 mM HEPES, pH 7.4). Patch pipettes were prepared by pulling micro-hematocrit capillary tubes (OD 1.50–1.60 mm) (Garner Glass Co., Claremont, CA, USA) using a needle/pipette puller (Model PP-83, Narishige, Japan), fired polished, and coated with Sylgeard (Dow-Corning, Midland, IL, USA). The pipettes' input resistance varied between 2 and 5 MΩ when filled with an internal solution (150 mM KCl, 10 mM HEPES, 3 mM EGTA, 3 mM sucrose, pH 7.31). The pipettes were connected to the input stage of a patch-clamp amplifier (Axopatch 1-D; Axon Instruments Inc., Union City, CA, USA). Currents were filtered although a low-pass 8-pole Bessel filter at 2 kHz, digitalized at 50–500 μs intervals and recorded using a Digidata 1200 D/A interface board and pClamp 6.04 software (Axon Instruments Inc.). Data were analyzed off-line with the aid of pClamp 8.02 and Origin 4.0 (Originlab Corp., Northampton, MA, USA). Each experiment was repeated three times on triplicate samples. 4-AP (Sigma) was

Table 1 Primers for $K_v3.4$ amplification

Pair	*Amplicon (bp)*	*Primer*	*Sequence*	*Nucleotide number*
1	1775	Sense	5′-CCGCAGCGCTTCTTATGATC-3′	143–1917
		Antisense	5′-AACACTTTGCCCTCATAAAGG-3′	
2	318	Sense	5′-CCTGCTGCTGGATGACCT-3′	581–898
		Antisense	5′-GGGTCTCCAGGCAGAAAGT-3′	

dissolved in dimethyl sulfoxide (DMSO). The IC_{50} of OECM-1 for 12 h treatment of 4-AP is 2 mM (18). 4-AP (2 mM) was either filled in the internal solution or applied into the extracellular perfusate to block the channel activity and confirm the specificity of the current.

MTT cell viability assay
The viability of cells cultivated on 24-well culture plates was measured by adding 3-(4′5-dimethylthiazol-2-yl)-2,5-diphenyltetrazolium bromide (MTT) reagent dissolved in phosphate-buffered saline (PBS), to a final concentration of 0.5 mg/ml. After 4 h of incubation, cells were solubilized in 0.5 N HCl, 5% Triton X-100, and 45% 2-propanol (final concentration). The intensity of dissolved formazan crystal was measured at 590 nm by an enzyme-linked immunosorbent assay (ELISA) reader. Responses that were not in dose-dependent and/or time-dependent manner were considered to be non-specific.

Foci formation assay
To assay transformability, 1000 3T3/K_v3.4 and control cells were seeded in 60 mm grid dishes. The cells grew 3–4 weeks to complete confluence. They were left in the wells and grown for 2 more weeks to allow foci formation. Control cells treated with 10 μg/ml benzo(a)pyrene (B(a)P; Sigma) for 6 weeks served as positive controls (20).

Statistical analysis
The *t*-test was used for analysis. Differences between the values were considered significant when $P < 0.05$.

Results

Generation of cells stably expressing $K_v3.4$
The plasmid, pcDNA3.1/K_v3.4, was sequenced to know the correct K_v3.4 cDNA insert. It was transfected to OECM-1 and 3T3 cells. The empty vector pcDNA3.1 was also transfected to establish control cells. The distinctive clones containing stable exogenous K_v3.4 cDNA were named OECM-1/K_v3.4 and 3T3/K_v3.4. The control cells were OECM-1/neo and 3T3/neo. Figure 1a depicts the presence of a K_v3.4 cDNA in the genomic DNA from variable OECM-1/K_v3.4 clones, indicating the integration of plasmids in contrast to controls. Figure 1b shows strong expression of exogenous K_v3.4 cDNA in variable OECM-1/K_v3.4 clones in contrast to control cells which exhibit weaker endogenous K_v3.4 mRNA expression. OECM-1/K_v3.4 clones S1–S4 as well as OECM-1/neo clones C1 and C2 were used for subsequent analysis. 3T3/K_v3.4 clones S1 and S2 expressing exogenous K_v3.4 cDNA together with 3T3/neo control clones C1 and C2 were subjected to subsequent experiments.

OECM-1/$K_v3.4$ produced functional A-type K_v
Figure 2a–c shows a representative example of membrane currents in OECM-1/K_v3.4 clone S3 cells (a and b) and in a control OECM-1/neo clone C1 cells (c). Both

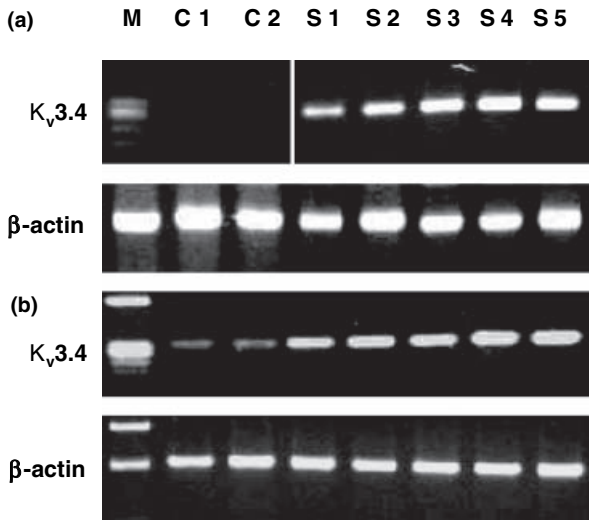

Figure 1 Integration and constitutive expression of exogenous K_v3.4 cDNA in OECM-1/K_v3.4 cells. (a) Polymerase chain reaction (PCR) reaction using genomic DNA as the template to produce 318 and 621 bp amplicons for K_v3.4 (upper panel) and β-actin (lower panel), respectively. No amplicon was generated in control clones C1 and C2. Distinctive amplicons were generated in OECM-1/K_v3.4 clones S1–S5, indicating the integration of K_v3.4 cDNA in the genome. (b) Reverse transcriptase (RT)-PCR reaction using cDNA as template to produce amplicons for K_v3.4 (upper panel) and β-actin (lower panel). The PCR cycle number was limited to lower range of linear amplification to distinguish the difference of K_v3.4 mRNA expression in variable clones. Faint amplicons were generated in control clones C1 and C2. Distinctive amplicons were generated in OECM-1/K_v3.4 clones S1–S5, indicating the expression of exogenous K_v3.4 cDNA in various clones.

clones of cell displayed an A-type channel pattern. However, between the cells, a substantial difference exists in the activation rate, the amplitude of current and the inactivation rate. The normalized currents (Fig. 2d) showed the inactivation of K_v3.4 (at +100 mV) in OECM/K_v3.4 clone S3 and OECM/neo clone C1. It denotes a slower inactivation in OECM-1/K_v3.4 clone S3 cells than that in OECM-1/neo clone C1 cells all the time following the currents reached peak. In addition, the difference in the activation time to the peak in OECM-1/K_v3.4 clone S3 cells and OECM-1/neo clone C1 cells, was calculated to be 1.85 ms and 0.55 ms, respectively. The results further implied the presence of a unique A-type K_v in OECM-1 cells expressing exogenous K_v3.4.

We performed a further investigation if 4-AP specifically block the A-type K_v using OECM-1/K_v3.4 clone S4 cells. The potassium currents of these cells were initially elicited by holding the membrane potential at −100 mV and then stimulating the cell for 80 ms from −100 to +100 mV in 10 mV increments. Outward currents were transient and inactivated within 30–50 ms. In addition, these outward currents were activated at potentials which were more positive than −10 mV and increased with increasing voltages (Fig. 3d). The activated outward currents tended to be inactivated rapidly at more positive potential (Fig. 3a,c). When 2 mM 4-AP was perfused into the bath, the transient outward currents were abolished

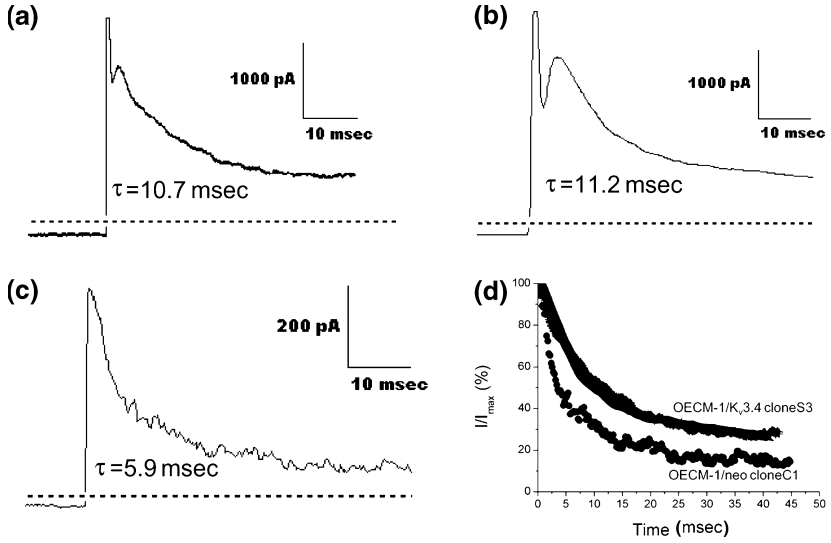

Figure 2 The A-type K_v in OECM-1/K_v3.4 cells and OECM-1/neo control cells. Current traces measured after stimulating the cells for 45 ms starting from a holding potential of −100 mV to +90 mV. (a and b) OECM-1/K_v3.4 clone S3 cells (sampling rate = 20 kHz). In the initial phase, there are two components of capacitive currents caused by the potential changes across the pipette (fast) and cell membrane (slow) in the absence of cancellation. A-type K_v current appeared right after these capacitive currents relaxed. (c) OECM-1/neo clone C1 cells, a more rapid activation current (sampling rate = 5 kHz) with a lower amplitude and a rapid inactivation rate was noted in this cell. (d) The illustration marks the peak residual activated current vs. time lapse following the initiation of inactivation. A remarkable difference between OECM-1/K_v3.4 clone S3 cells and OECM-1/neo clone C1 cells was noted. The dot lines represented zero current level. The results shown are representatives of two independent experiments.

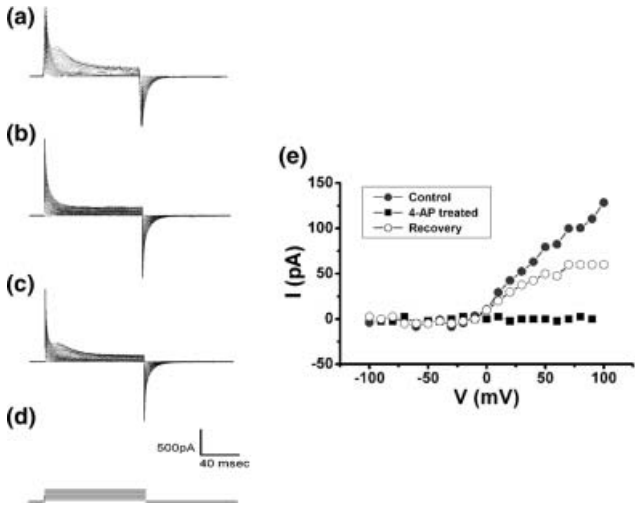

Figure 3 The A-type K_v in OECM-1/K_v3.4 cells. Current traces were recorded in the cells depolarized from a holding potential of −100 mV to various potentials ranging from −100 to +100 mV in 10-mV increments. In the initial phase, capacitive currents were presented. A-type K_v current appeared right after these capacitive currents relaxed. (a) OECM-1/K_v3.4 clone S4, uniform, transient A-type current is recorded. (b) Complete absence of the current throughout treatment with 2 mM 4-aminopyridine (4-AP). (c) Partial recovery of the A-type channel activity obtained by washing 4-AP out. (d) Voltage protocols for measuring A-type K_v. (e) The illustration of the peak current vs. stimulatory potential recorded in control, 4-AP-treated, and recovery OECM-1/K_v3.4 clone S4 showing the functional presence of an A-type K_v. The results shown are representative of two independent experiments.

(Fig. 3b); eliminating 4-AP treatment led to recovery (Fig. 3c). This relationship is more discernable in the current–voltage plot in Fig. 3e, in which peak current

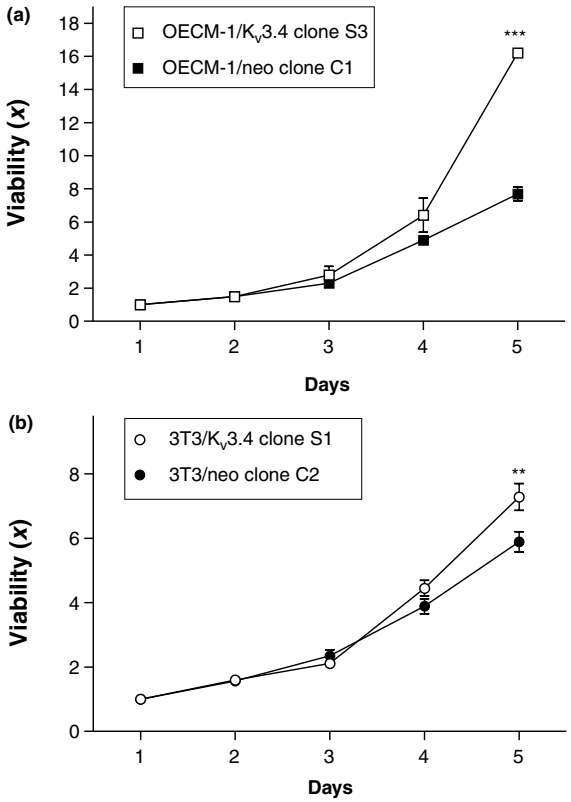

Figure 4 Proliferation of OECM-1/K_v3.4 and control cells. (a) Significant difference in cell viability between OECM-1/K_v3.4 clone S3 and control clone C1 on the fifth day of culture. (b) A slight increase in the cell viability of 3T3/K_v3.4 clone S1 relative to control clone C1. $^{**}P < 0.01$, $^{***}P < 0.001$. The results are the mean ± SE for three to five separate experiments.

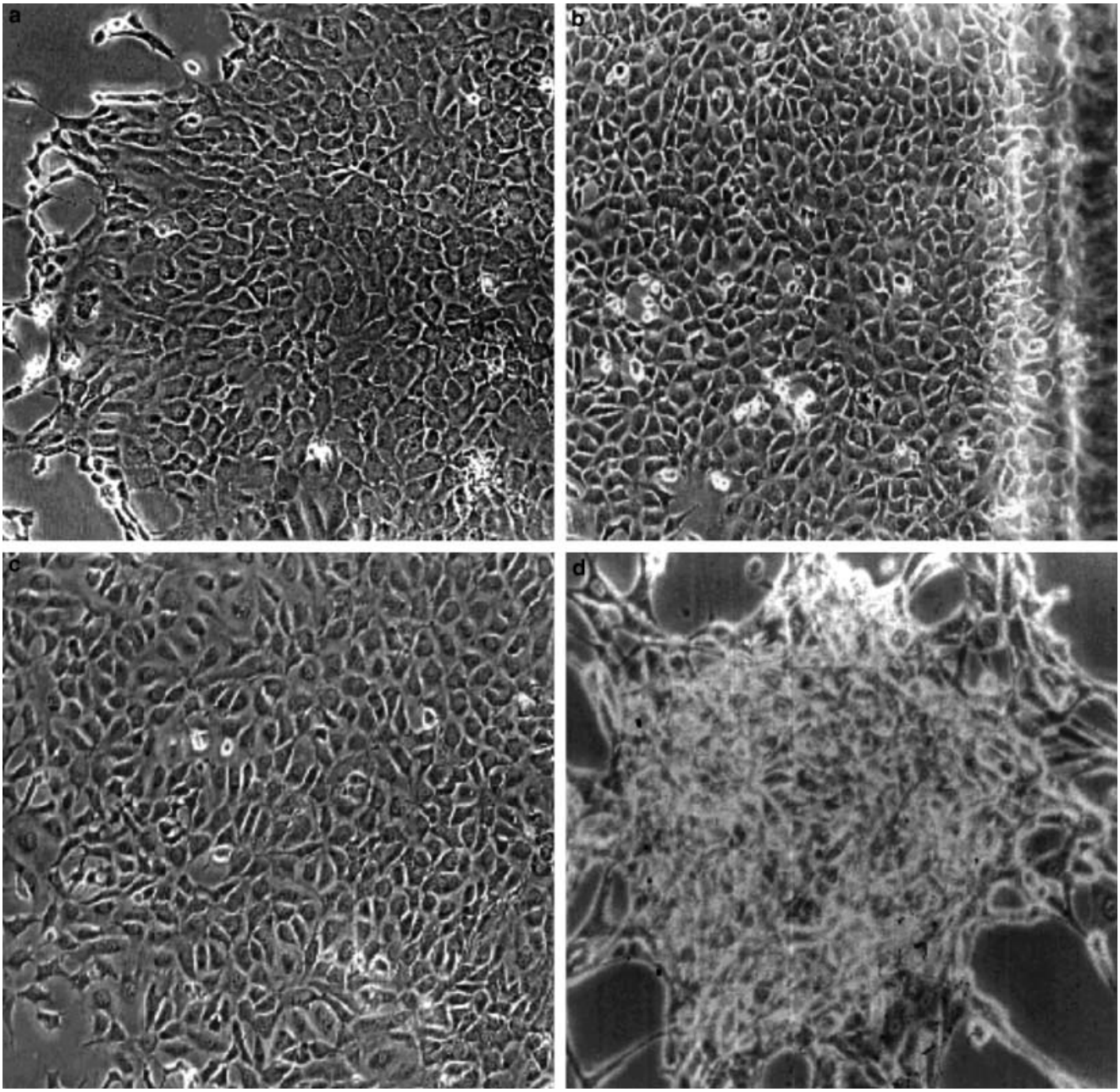

Figure 5 3T3/K_v3.4 and foci formation. (a and b) Individual 3T3/K_v3.4 cell clones S1 and S2 at third to fourth week of culture show no foci formation. (c) Control 3T3/neo clone C1 shows no foci formation at the fourth week of culture. (d) A control 3T3/neo clone C1 with 10 μg/ml benzo(a)pyrene [B(a)P] treatment for 4 weeks shows foci formation. The results shown are representative of two independent experiments.

amplitudes were arrayed as a function of applied potentials. Overall, the electrophysiological findings imply the existence of a functional A-type K^+ channel in OECM-1/K_v3.4 clone S4 cells through the over-expression of exogenous K_v3.4 cDNA.

Expression of $K_v3.4$ advantageous for proliferation of OECM-1

To confirm the involvement of K_v3.4 function in the proliferation of oral keratinocytes, cell viability was analyzed. The increase in viability was defined by MTT value at day 10 to MTT value at day 0. As shown in Fig. 4a, OECM-1/K_v3.4 clone S3 cells had a slightly higher viability when comparing with a control clone of C1 cells in the first 4 days of culture. However, the difference was not statistically significant. A considerable difference in the viability was observed in the fifth day, showing that OECM-1/K_v3.4 clone S3 was increased for approximately 120% when compared with that of control clone C1 cells ($P < 0.001$, *t*-test). Approximately 70% increase of viability for OECM-1/K_v3.4 clone S4 cells compared with control clone C2 cells was also noted at the end of the exponential growth phase. In the fifth day, 3T3/K_v3.4 cell clones had an

increased proliferation rate of approximately 32% in clones S1 relative to 3T3/neo clones C1 (Fig. 4b) and approximately 28% in clones S2 relative to C2 ($P < 0.05$, *t*-test).

Foci formation in 3T3 cells

Figure 5a–c shows 3T3/K_v3.4 clones S1 and S2 (a and b) and a 3T3/neo clone C1 (c). 3T3/K_v3.4 cell clones ceased growing when a homogeneous monolayer covered the plate. No foci formation was noted during extended culture after confluence for 2 more weeks. However, the control cells formed numerous foci with different sizes when treated with 10 μg/ml B(a)P for a duration of 4 weeks. The cells in foci exhibited characteristic transformation features including spindle-shape morphological change, loss of contact inhibition, and piling up (Fig. 5d). To assure the stable integration of K_v3.4 plasmid in 3T3/K_v3.4 clones, these cells were re-selected using geneticin for 1 more week. The absence of cytotoxicity observed indicated the presence of plasmid in cells.

Discussion

Except for EAG K_v, which has been proposed as a link between tumorigenesis of epithelial cell and K^+ channel activity, very few papers have documented the contribution of K_v in the pathogenesis of epithelial cells (12). In a previous study, we have provided tissue evidences that K_v3.4 mRNA overexpressed in a large fraction of OSCC and ESCC tissue (18). The high incidence of K_v3.4 mRNA expression in SCC suggests that it might be involved in tumorigenesis of keratinocytes. In this study, a K_v3.4 transfectant was established to identify the impacts of K_v3.4 on cellular phenotypes (Fig. 1). Although the protein evidences were not available due to the lack of appropriate antibody, the OECM-1 oral keratinocyte cells constitutively expressed exogenous K_v3.4 cDNA and displayed a unique A-type current similar to the K_v3.4 indicating the presence of functional channel (Fig. 2). The pharmacological sensitivity of such current to 4-AP further supported the presence of functional channel activity (Fig. 3).

Comparing with controls, OECM-1 cells carrying constitutive expression of exogenous K_v3.4 had an increase in growth for about a fold at the end-point of exponential growth (Fig. 4a). The role of the K^+ channel in cell proliferation has been interpreted as controlling the cell volume via the K^+ concentration, influencing intracellular Ca^{++} concentration, or interacting with other cellular molecules (1, 6–8). It has been shown that actively proliferating cells such as tumor cells had more depolarizing membrane potential (17). Although it is still not understood how K_v3.4 channel activity influences cell proliferation, our experiments might support the speculation that K_v3.4 current is involved in maintaining the depolarized membrane potential required for cancer cells (3). The oncogenomic events regulating the expression or activation of K_v3.4 are to be determined.

It was notable that cellular transformation by oncogenes *Ras* and *Src*; and oncoviruses RSV and SV40 increased K^+ channel activity (22–25). The injection of cells constitutively expressed EAG K_v induces transformed phenotypes in immunodeficient mice (12). We found that the overexpression of K_v3.4 could be a common feature of SCC, however, we were unable to achieve a transformed phenotype in 3T3/K_v3.4 fibroblasts (Fig. 5). This disparity was due most likely to the insufficient acquisition of growth advantage in the 3T3 cells expressing K_v3.4 (Fig. 4b). Whether the K_v3.4 function is cell type-specific requires further study. Alternatively, K_v3.4 may confer a growth advantage only in neoplastic cells but not in non-transformed cells. Otherwise, the K_v3.4 might not be transformation-associated. Efforts are underway to distinguish these possibilities by selecting highly proliferative 3T3/K_v3.4 cell clones first.

In summary, we demonstrated the novel findings of the involvement of K_v3.4 activity in the growth of an OSCC cell line. The transfectant system established can be further employed to explore the contribution of K_v3.4 activity in additional phenotypes advantageous for neoplastic process. As K_v3.4 is frequently overexpressed in OSCC, it is postulated that the blockage of functional K_v3.4 will intercept the growth of OSCC.

References

1. Jan LY, Jan YN. Cloned potassium channels from eukaryotes and prokaryotes. *Annu Rev Neurosci* 1997; **20**: 91–123.
2. Rudy B, Sen K, Vega-Saenz de Miera E, Lau D, Ried T, Ward DC. Cloning of a human cDNA expressing a high voltage-activating, TEA-sensitive, type-A K^+ channel which maps to chromosome 1 band p21. *J Neurosci Res* 1991; **29**: 401–12.
3. Cayabyab FS, Schlichter LC. Regulation of an ERG K^+ current by Src tyrosine kinase. *J Biol Chem* 2002; **277**: 13673–81.
4. Cayabyab FS, Tsui FW, Schlichter LC. Modulation of the ERG K^+ current by the tyrosine phosphatase, SHP-1. *J Biol Chem* 2002; **277**: 48130–8.
5. DeCoursey TE, Chandy KG, Gupta S, Cahalan MD. Voltage-gated K^+ channels in human T lymphocytes: a role in mitogenesis? *Nature* 1884; **307**: 465–8.
6. Yao X, Kwan HY. Activity of voltage-gated K^+ channels is associated with cell proliferation and Ca2+ influx in carcinoma cells of colon cancer. *Life Sci* 1999; **65**: 55–62.
7. Pancrazio JJ, Tabbara IA, Kim YI. Voltage-activated K^+ conductance and cell proliferation in small-cell lung cancer. *Anticancer Res* 1993; **13**: 1231–4.
8. Nilius B, Wohlrab W. Potassium channels and regulation of proliferation of human melanoma cells. *J Physiol* 1992; **445**: 537–48.
9. Bianchi L, Wible B, Arcangeli A, et al. herg encodes a K^+ current highly conserved in tumors of different histogenesis: a selective advantage for cancer cells? *Cancer Res* 1998; **58**: 815–22.
10. Cherubini A, Taddei GL, Crociani O, et al. HERG potassium channels are more frequently expressed in

human endometrial cancer as compared to non-cancerous endometrium. *Br J Cancer* 2000; **83**: 1722–9.
11. Smith GA, Tsui HW, Newell EW, et al. Functional up-regulation of HERG K^+ channels in neoplastic hematopoietic cells. *J Biol Chem* 2002; **277**: 18528–34.
12. Pardo LA, del Camino D, Sanchez A, et al. Oncogenic potential of EAG K^+ channels. *EMBO J* 1999; **18**: 5540–7.
13. Camacho J, Sanchez A, Stuhmer W, Pardo LA. Cytoskeletal interactions determine the electrophysiological properties of human EAG potassium channels. *Pflugers Arch* 2000; **441**: 167–74.
14. Stringer B, Cooper A, Shepard S. Overexpression of the G-protein inwardly rectifying potassium channel 1 (GIRK1) in primary breast carcinomas correlates with axilliary lymph node metastasis. *Cancer Res* 2001; **61**: 582–8.
15. Abbott G, Butler M, Bendahhou S, Dalakas M, Ptacek L, Goldstein S. MiRP2 forms potassium channels in skeletal muscle with $K_v3.4$ and is associated with periodic paralysis. *Cell* 2001; **104**: 217–31.
16. Antz C, Bauer T, Kalbacher H, et al. Control of K^+ channel gating by protein phosphorylation: structural switches of the inactivation gate. *Nat Struct Biol* 1999; **6**: 146–50.
17. Wonderlin WF, Strobl JS. Potassium channels, proliferation and G1 progression. *J Memb Biol* 1996; **154**: 91–107.
18. Chang KW, Yuan TC, Fang KP, Yang FS, Liu CJ, Lin SC. The increase of voltage-gated potassium channel $K_v3.4$ mRNA expression in oral squamous carcinoma. *J Oral Pathol Med* 2003; **32**: 205–11.
19. Lin SC, Wang CP, Chen YM, et al. Regulation of IGFBP-5 expression during tumorigenesis and differentiation of oral keratinocytes. *J Pathol* 2002; **198**: 317–25.
20. Lo KY, Kakunaga T. Similarities in the formation and removal of covalent DNA adducts in benzo(a)pyrene-treated BALB/3T3 variant cells with different induced transformation frequencies. *Cancer Res* 1982; **42**: 2644–50.
21. Keyomarsi K, Sandoval L, Band V, Pardee AB. Synchronization of tumor and normal cells from G1 to multiple cell cycles by lovastatin. *Cancer Res* 1991; **51**: 3602–9.
22. Huang Y, Rane SG. Potassium channel induction by the Ras/Raf signal transduction cascade. *J Biol Chem* 1994; **269**: 31183–9.
23. Repp H, Draheim H, Ruland J, et al. Profound differences in potassium current properties of normal and Rous sarcoma virus-transformed chicken embryo fibroblasts. *Proc Natl Acad Sci USA* 1993; **90**: 3403–7.
24. Draheim HJ, Repp H, Dreyer F. Src-transformation of mouse fibroblasts induces a Ca^{++}-activated K^+ current without changing the T-type Ca^{++} current. *Biochem Biophys Acta* 1995; **1269**: 57–63.
25. Teulon J, Ronco PM, Geniteau-Legendre M, et al. Transformation of renal tubule epithelial cells by simian virus-40 is associated with emergence of Ca^{++}-insensitive K^+ channels and altered mitogenic sensitivity to K^+ channel blockers. *J Cell Physiol* 1992; **151**: 113–25.

Acknowledgments

Authors acknowledge Ms Fen-Lin Chen for her assistance. Supported by National Research Program for Genomic Medicine grant 91GMP004-3 and National Science Council grant NSC 91-3112-B010-005, Taiwan.